10.1109/ULTSYM.2014.0551

Bistatic passive mapping of the field distribution of single element transducer in agar phantom

Trong Nguyen, Michael Oelze, and Minh Do

***Abstract*—High intensity focused ultrasound (HIFU) can provide a means of noninvasive ablation or hyperthermia of tissues such as tumors. Real-time monitoring of the progression of the field distribution of the HIFU transducer during treatment is important for localizing the intersection of the beam with the tissue. By continuously visualizing the HIFU field in a tissue, better positioning of the HIFU beam for therapy can be obtained during treatment. To visualize the HIFU field in a tissue, a passive listening technique was employed using beamforming approaches and a linear array system co-aligned with the HIFU source. The passive array made use of the weakly scattered signal from the medium to reconstruct the field pattern of the HIFU field in the medium.**

The focus of a 6-MHz single-element transducer (f/3) was aligned perpendicular to the field of view from a linear array (L14-5) operated by a SonixRP system equipped with a SonixDAQ. A homogeneous tissue-mimicking phantom made of agar containing glass beads was placed at the focus between the 6-MHz source and the linear array. The 6-MHz source was excited with a pulse and the field scattered from the phantom was received by each element of the linear array. Beam forming techniques were used to focus the received field of the linear array around the focal region of the 6-MHz source. The intensity field pattern of the 6-MHz source was reconstructed from the scattered field. Next, a wire target was placed in the field and the intensity field pattern was reconstructed by moving the wire throughout the focal region. The intensity pattern from the phantom was compared to the nominal field characteristics of the 6-MHz source and to the field characterized by a wire.

The beam width at the focus of the reconstructed intensity field pattern was estimated to be 1.7 mm. The nominal estimate of the beam width was approximately 1.4 mm (-6 dB) and the beam width as estimated from the wire target field mapping was 1.5 mm. Therefore, the novel passive reconstruction technique can visualize the field of a focused source in a weakly scattering medium.

***Index Terms*—passive mapping, beamforming**

I. Introduction

High intensity focused ultrasound (HIFU) allows noninvasive ablation or hyperthermia of tissue such as tumors. Real-time monitoring of the HIFU beam allows for better positioning and can help prevent adverse effects in normal tissue. In this study, a passive mapping technique is presented that allows the field of the HIFU source to be reconstructed and superimposed on a B-mode image of the medium.

A pulse excitation of the HIFU source will result in scattered wavelets from the tissue or medium. A passive linear array co-aligned with the HIFU source beam will receive the scattered field. Assuming uniform scattering in the medium, the intensity pattern of the scattered field will follow the field intensity of the HIFU beam. Therefore, a representation of the HIFU beam can be reconstructed from the scattered field through passive mapping with the linear array. Passive mapping of the HIFU beam using a passive listening array allows for continuous feedback of the progression of the interaction of the beam with the tissue [1], [2]. When the HIFU transducer and the passive listening array are not co-located, a bistatic beamforming technique is employed to accurately map the transmit-receive field.

This study presents a novel passive listening technique where the transmitting transducer and the receiving array are perpendicular to each other. The transmit-receive field of the system was characterized by a tungsten wire. The passive listening technique was later used to reconstruct the intensity pattern of the transmitting transducer in an agar phantom with glass beads.

II. Methods

A. Characterizing the transmit-receive field of the setup using a wire

A tungsten wire with a diameter of 38 μm was placed at the focus of a 6-MHz f/3 single-element transducer. Since the beamwidth of the single element was only 1.4 mm, a special holder was made to align the single element beam and the imaging plane of the receiving array. The holder, which holds the single element transducer and the array, was connected to a micro-precision positioning system (Daedal Inc. Harrison City, PA). The wire was moved through the focal region of the single-element with an axial dimension of 20 mm and lateral dimension of 1 mm. The scanning grid was centered at the focus of the single-element transducer. The axial scanning step was 0.5 mm and the lateral scanning step was 0.1 mm. For each step, the single-element transducer was excited using a Panametrics 5800 pulser-receiver (Olympus NDT, Waltham, MA). The scattered signal was received by the linear array (L14-5) operated by the SonixRP system equipped with a SonixDAQ (Ultrasonix Medical Corp., Richmond, BC, Canada). The excitation onset of the single-element transducer and the receiving onset of the linear array were synchronized. The pre-beamformed data acquired by the SonixDAQ were downloaded to a hard-drive for post processing.

B. Tissue phantom field reconstruction

An agar-based phantom filled with glass beads was used to simulate tissue in this study. After characterizing the system using the wire, the wire positioned at the focus of the single-element transducer was replaced by the phantom. The single-element transducer was excited by the 5800 and the scattered signal was recorded by the linear array. The phantom was

translated laterally with a 0.2 mm step to capture different realizations of the field. Five consecutive snapshots were used to form a reconstructed compounded image. The same delay-estimation procedure was carried out. The setup of the agar phantom experiment is shown in Fig. 1.

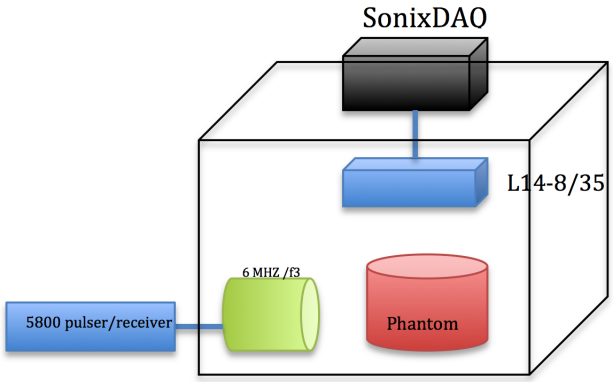

Fig. 1: Experiment setup.

To visualize the relative position of the reconstructed beam, the B-mode image of the phantom was taken with the SonixRP built-in software while the single-element transducer excitation was turned off. The reconstructed beam of the single-element transducer in the agar phantom was overlaid on the B-mode image.

Due to the bistatic nature of the setup, two delay estimation procedures were performed to correctly localize the beam. The first delay, due to the signal traveling from the single-element transducer to the wire/agar phantom, was estimated using the pulse-echo signal received by the 5800 pulser/receiver. This delay was subtracted from the receiving image of the array. A second delay was estimated to correct for the skew of the beam field due to the geometry of the array.

Delay-and-sum beamforming was used to reconstruct a B-mode image of the imaging target. For the wire, the passive map was generated by summing all beamformed images of the wire.

C. Delay-and-sum beamforming

The received data from the SonixDAQ consists of 128 channels of prebeamformed data, corresponding to 128 array elements. For each pixel (x_f, z_f) in the beamformed image, the delay time from other channels was calculated as follows:

$$t(i) = \frac{\sqrt{(x_f - x_i)^2 + (z_f - z_i)^2}}{c}, \quad (1)$$

for $i = 1, 2, .., 128$, where (x_i, z_i) is the coordinate of the array element i, (x_f, z_f) is the coordinate of the focused point, and c is the speed of sound.

The beamformed pixel value was calculated as follows:

$$I(x_f, z_f) = \sum_{i=1}^{128} s_i \left[z_f/c - t(i) \right], \quad (2)$$

where $s_i[n]$ is the channel data at the element i. The delayed sample usually was not an integer, thus linear interpolation between the two closest integer samples was used to compute the added value.

D. Delay compensation

The beamformed image is shown in Fig. 2 (a). The appearance of an incline in the beamformed field comes from the different delays experienced by the elements of the array and the orientation of the transmitting transducer relative to the array. The element closest to the single-element transducer will receive the scattered signal first. As an approximate delay compensation, these delays were calculated based on the pitch of the array. Two consecutive elements will experience a delay of $\tau = \Delta d/c$ where c is the speed of sound, and Δd is the pitch of the linear array. Correcting for the delays requires an angular transform, which will reorient the beam parallel to the linear array face (see Fig. 2b).

III. Results

Fig. 2 shows the passive map generated by moving the wire through the focus region of the single element. The right figure is the delay-corrected image of the left figure. Since the delay correction is an approximate process, we use Fig. 2 to estimate the -6-dB beamwidth of the single element. A red ellipse was drawn on the left figure to visualize the -6-dB beam. The -6-dB beamwith was estimated to be 1.5 mm. Fig. 2 (b) is not a rotated image of Fig. 2 (a) but rather a sheared image of Fig. 2 (a).

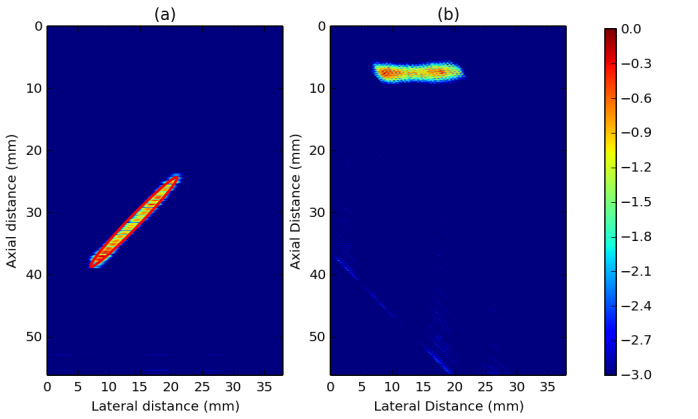

Fig. 2: Passive map of the focused field of the wire (a) before and (b) after correction.

Fig. 3 shows the beamformed image of the beam reconstructed from the phantom. Fig. 3 (a) is the beamformed image of a one transmit-receive event. Fig. 3 (b) shows the compounded image using five consecutive snapshots. Fig. 3 (c) is the corrected image of Fig. 3 (b). As in the case of the wire, the beamwidth was estimated using the pre-corrected beamformed image. The -3-dB beamwidth was difficult to estimate from the phantom image, thus the -6-dB beamwidth was estimated instead. The -6-dB beamwidth estimate was 1.7 mm.

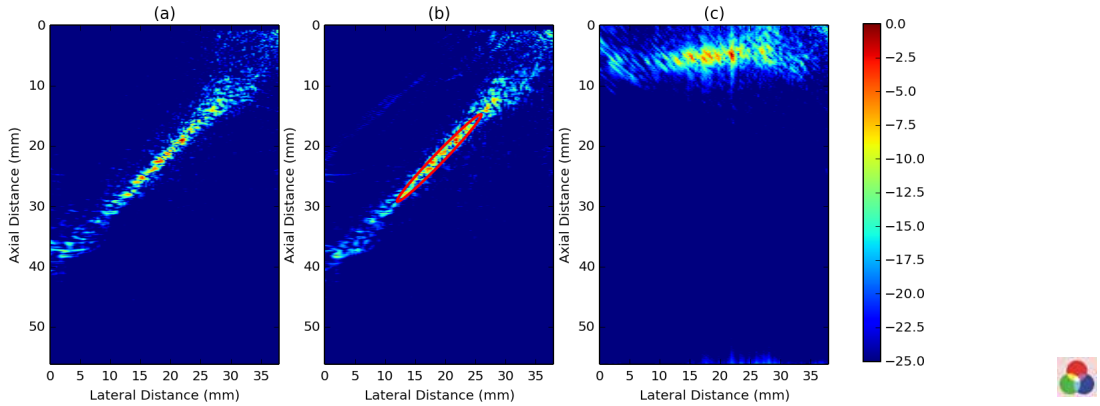

Fig. 3: (a) Beamformed image of one transmit-receive event. (b) Beamformed image of the beam in the phantom by compounding five transmit-receive events. (c) Delay-corrected image of Fig. 3 (b).

	Wire target	Agar phantom
Beamwidth	1.5 mm	1.7 mm
Depth-of-field	19 mm	20.1 mm

TABLE I: Comparison between the wire target and agar phantom -6-dB beamwidth and depth of field.

Fig. 4 shows the position of the delay-corrected compounded beam of the single element overlaid on the B-mode image. Table I compares the beamwidth and depth of field (DOF) as estimated from the wire target and phantom target beamformed data.

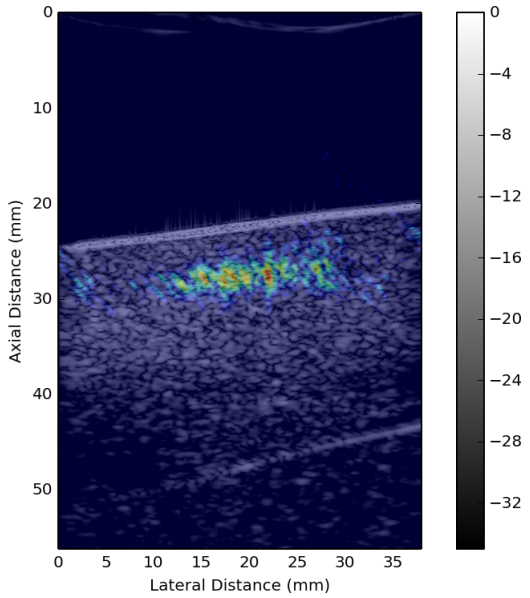

Fig. 4: Passive map of the field of Fig. 3 (c) overlaid on the B-mode image.

IV. Discussion

A novel passive mapping technique was demonstrated that allowed the reconstruction of the beam field, and this corresponded well to a simple wire target. The nominal -6-dB beamwidth of the single-element transducer was 1.4 mm, the -6-dB beamwidth estimate from the wire target mapping was 1.5 mm.

The passive mapping of scatterers in the agar phantom was equivalent to the wire mapping except the whole field throughout the beam could be acquired at one excitation. Using the scattering reconstruction technique, the -6-dB beamwidth was estimated to be 1.7 mm. The -3-dB could not be estimated due to the discontinuity of the reconstructed field.

Compounding appeared to smooth out the representation of the field. Compounding also helped increase the signal to noise ratio and eased the estimation of the -6-dB beamwidth. The -6-dB beamwidth representation was not continuous but rather appeared as a speckle pattern. Therefore, the more images used in the compounding, the clearer the pattern of the beam emerged.

The reconstructed field could be superimposed on B-mode images to give anatomical context of the location of the HIFU beam in a tissue. Furthermore, bright spots in the corresponding B-mode image could be used to correct for image intensity variations in the field pattern due to structures in the tissues like bright specular scatterers or tissue interfaces.

The pre-beamformed data was processed offline due to the capabilities of the SonixDAQ. The beamforming code written in Python was sequential and took about 40 seconds. The code can be parallelized because the beamforming of each channel is independent of the other. Therefore, real-time visualization is a realizable goal.

V. Conclusions

This paper presents a passive mapping technique for the bistatic setup where the transmit transducer and receiving array were perpendicular to each other. It can be applied to map out the beam of a HIFU source *in situ* and for real-time monitoring and feedback for treatment of tumors.

References

[1] V. A. Salgaonkar, S. Datta, C. K. Holland, and T. D. Mast, "Passive cavitation imaging with ultrasound arrays," *The Journal of the Acoustical Society of America*, vol. 126, no. 6, pp. 3071–3083, 2009.

[2] M. Gyongy and C.-C. Coussios, "Passive spatial mapping of inertial cavitation during hifu exposure," *Biomedical Engineering, IEEE Transactions on*, vol. 57, no. 1, pp. 48–56, 2010.